A&A 433, 415–429 (2005)
DOI: 10.1051/0004-6361:20041870

Astronomy & Astrophysics

RASS-SDSS galaxy cluster survey

II. A unified picture of the cluster luminosity function

P. Popesso[1], H. Böhringer[1], M. Romaniello[2], and W. Voges[1]

[1] Max-Planck-Institut fur extraterrestrische Physik, 85748 Garching, Germany
e-mail: popesso@mpe.mpg.de
[2] European Southern Observatorty, Karl Scharzschildstr. 2, 85748 Garching b. München, Germany

Received 20 August 2004 / Accepted 1 December 2004

Abstract. We constructed the composite luminosity function (LF) of clusters of galaxies in the five SDSS photometric bands u, g, r, i and z from the RASS-SDSS galaxy cluster catalog. Background and foreground galaxies are subtracted using both a local and a global background correction to take in account the presence of large scale structures and field to field variations, respectively. The composite LF clearly shows two components: a bright-end LF with a classical slope of –1.25 in each photometric band, and a steeper faint-end LF ($-2.1 \leq \alpha \leq -1.6$) in the dwarf galaxy region. The observed upturn of the faint galaxies has a location ranging from $-16 + 5\log(h)$ in the g band to $-18.5 + 5\log(h)$ in the z band. To study the universality of the cluster LF we compare the individual cluster LFs with the composite luminosity function. In agreement with the composite LF, a single Schechter component is not a good fit for the majority of the clusters. We fit a Schechter function to the bright-end of the individual cluster LFs in the magnitude region brighter than the observed upturn of the dwarf galaxies. The bright-end of the galaxy clusters shows the same shape in all the systems. To study the behavior of the individual faint-end LF we define the Dwarf to Giant galaxy Ratio (DGR) of the single clusters. The distribution of DGR has a spread much larger than the statistical errors. The DGR clearly anti-correlates with both X-ray and optical cluster luminosities. This anti-correlation is most likely due to the choice of a fixed metric aperture for all the clusters. Therefore, because of this effect, the different cluster physical sizes must be taken into account before comparing the LF of different clusters.

Key words. galaxies: clusters: general – galaxies: general

1. Introduction

The galaxy luminosity function (LF) is one of the most direct observational test of theories of galaxy formation and evolution. Clusters of galaxies are ideal systems within which to measure the galaxy LF for the large number of galaxies at the same distance. There are two main purposes for the study of the cluster LF: the comparison of the galaxy LF in clusters and field and thus the study of the influence of the environment on the global statistical properties of galaxies, and the search for differences in the LF of different clusters as indicators of differences in the galaxy formation due to environmental effects or dynamical processes.

The cluster galaxy over-density with respect to the surrounding field is sufficiently high to efficiently identify members either photometrically through the statistical removal of foreground and background galaxies or spectroscopically. These techniques have been used to measure LFs for individual clusters or to form a composite LF, in order to eliminate the peculiarity of the individual LFs and enhance the underlying possibly universal LF (Dressler 1978; Lugger 1986; Colless 1989; Lugger 1989; Lumsden et al. 1997; Valotto et al. 1997; Rauzy et al. 1998; Garilli et al. 1999; Paolillo et al. 2001; Goto et al. 2002b; Yagi et al. 2002). Many of these studies do not agree on the exact form of the LF. Several authors (Dressler 1978; Lumdsen 1997; Valotto et al. 1997; Garilli et al. 1999; Goto et al. 2002b) found differences between the LFs of different clusters and between cluster and field, while others (Lugger 1986; Colless 1989; Lugger 1989; Rauzy 1998; Trentham 1998; Paolillo et al. 2001) concluded that the galaxy LF is universal in all environments. However, all these works used different techniques and selections to check the universality of the cluster LF. Therefore, it is difficult to understand if their conclusions depend on the different tests beeing applied or to actual physical distinctions. Table 1 summarizes the variations between previous studies in the same color and their σ error limits for the Schechter parameters M^* and α. We have transformed magnitudes to $H_0 = 100\,\mathrm{km\,s^{-1}\,Mpc^{-1}}$ without changing their cosmology.

So far, the majority of the studies on the cluster composite LF has concentrated on the slope at the relatively bright end of the cluster LF ($M_g \leq -17$) without taking into account the behavior of the dwarf galaxy population in clusters. Instead, much work has been done in recent years in measuring the faint

Table 1. Schechter parameters fitted to the Composite LF retrieved in the literature.

Reference	M^*	α	Band	Ncluster	Luminosity range
Goto et al. (2002b)	-20.84 ± 0.26	-1.40 ± 0.11	u	204	$-24 \leq M_u \leq -18$
Schechter (1976)	-19.9 ± 0.50	-1.24	b_j	13	$-22.5 \leq M_{b_j} \leq -18.5$
Dressler (1978)	-19.7 ± 0.50	-1.25	F	12	$-23.5 \leq M_F \leq -18.5$
Colless (1989)	-20.10 ± 0.07	-1.25	b_j	14	$-22.5 \leq M_{b_j} \leq -17$
Lumsden et al. (1997)	-20.16 ± 0.02	-1.22 ± 0.04	b_j	46	$-21 \leq M_{b_j} \leq -18$
Valotto et al. (1997)	-20.00 ± 0.10	-1.40 ± 0.10	b_j	55	$-21 \leq M_{b_j} \leq -17$
Rauzy et al. (1998)	-20.91 ± 0.21	-1.50 ± 0.11	b_j	28	$-21 \leq M_{b_j} \leq -17$
Garilli et al. (1999)	-20.30 ± 0.10	-0.94 ± 0.07	g	65	$-22.5 \leq M_{\rm g} \leq -15.5$
Paolillo et al. (2001)	-20.22 ± 0.15	-1.07 ± 0.08	g	39	$-24.5 \leq M_{\rm g} \leq -16.5$
Goto et al. (2002b)	-21.24 ± 0.11	-1.00 ± 0.06	g	204	$-24 \leq M_{\rm g} \leq -18$
De Propris et al. (2003)	-20.07 ± 0.07	-1.28 ± 0.03	b_j	60	$-22.5 \leq M_{b_j} \leq -16$
Lugger et al. (1989)	-21.31 ± 0.13	-1.21 ± 0.09	R	9	$-23 \leq M_R \leq -18.5$
Garilli et al. (1999)	-20.66 ± 0.16	-0.95 ± 0.07	r	65	$-22.5 \leq M_r \leq -15.5$
Paolillo et al. (2001)	-20.67 ± 0.16	-1.11 ± 0.08	r	39	$-24.5 \leq M_r \leq -16.5$
Yagi et al. (2002)	-21.30 ± 0.20	-1.31 ± 0.05	$R_{\rm C}$	10	$-23.5 \leq M_{R_{\rm C}} \leq -16$
Goto et al. (2002b)	-21.44 ± 0.05	-0.85 ± 0.03	r	204	$-24 \leq M_r \leq -18$
Paolillo et al. (2002)	-20.85 ± 0.20	-1.09 ± 0.11	i	39	$-24 \leq M_i \leq -17$
Goto et al. (2002b)	-21.54 ± 0.08	-0.70 ± 0.05	i	204	$-24 \leq M_i \leq -18$
Goto et al. (2002b)	-21.59 ± 0.06	-0.58 ± 0.04	z	204	$-24 \leq M_z \leq -18$

end ($-18 \leq M_{\rm g} \leq -10$) of the galaxy LF in several nearby clusters (e.g. Driver 1994; Smith et al. 1997; Phillipps et al. 1998; Boyce et al. 2001; Beijersbergen et al. 2001; Sabatini et al. 2002; Trentham 2003; Cortese et al. 2004). The LF of these clusters typically steepens faintward of about $M_{\rm g} \sim -18$ showing the debated upturn of the dwarf galaxies . The faint end slope α of the LF in this range of magnitudes typically lies in the range –1.4 to –2.2. Phillipps et al. (1998) noted that the steepness of the faint end slope appears to depend on the cluster density, with dwarfs being more common in lower density environments. This is possibly because the various dynamical processes which can destroy dwarf galaxies act preferentially in dense environments.

In this paper we present the analysis of the cluster composite LF based on the second release of the Sloan Digital Sky survey (SDSS DR2, Abazajian et al. 2004). The excellence of the SDSS DR2 in terms of its size, depth and sky coverage and the accurate photometry in 5 different optical wavebands gives unprecedented advantages in comparison to the previous studies. Firstly, the sky coverage (3324 deg^2) gives us the possibility to overcome the well-known problem of the statistical subtraction of the galaxy background. We used large areas of the survey to define a mean global galaxy background and a region close to the clusters to determine the local galaxy background in order to check for systematics in the field subtraction. Secondly, the apparent magnitude limit of the SDSS DR2 in all the five bands is sufficiently deep (e.g. $r_{\rm lim} = 22.2$, 95% completeness) that, at the mean redshift of our cluster sample ($z \sim 0.15$), the cluster LF can extend and cover a significant part of the dwarf region, going deeper than in all previous studies of the composite luminosity function (more than 6 mag fainter than M^*). Thirdly, the high accuracy of the SDSS photometry in all bands gives us the possibility to measure in a statistically significant way the individual cluster LF with the consequent opportunity to check directly the universality of the LF. Furthermore, the accurate multi-color photometry allows us to use several objectively-measured galaxy properties like galaxy morphology. Finally, our comparison of the cluster and field LFs can done within the SDSS data.

To calculate the cluster composite LF we used the RASS-SDSS galaxy cluster sample (Popesso et al. 2004), which includes 130 systems observed in X-rays. The use of the RASS-SDSS galaxy cluster catalog ensures that none of the systems is a simple projection of large scale structure along the line of sight.

The paper is organized as follows: in Sect. 2 we describe the properties of the cluster sample and the optical galaxy photometry; in Sect. 3 we explain the methods used in constructing the individual cluster LFs and the methods of the background subtraction, in Sect. 4 we describe the methods used for building the Composite LF, in Sect. 5 we describe in detail our results. Section 6 contains our conclusions. Throughout the paper we use $H_0 = 100$ km s^{-1} Mpc^{-1}, $\Omega_{\rm m} = 0.3$ and $\Omega_\lambda = 0.7$.

2. The data

The RASS-SDSS galaxy cluster catalog comprises 130 systems detected in the ROSAT All Sky Survey (RASS). The X-ray cluster properties and the cluster redshift have been taken from different X-ray catalogs: the ROSAT-ESO flux limited X-ray cluster sample (REFLEX, Böhringer et al. 2003), the Northern ROSAT All-sky cluster sample (NORAS, Böhringer et al. 2000), the NORAS 2 cluster sample (Retzlaff 2001), the ASCA Cluster Catalog (ACC) from Horner et al. (2001) and

the Group Sample (GS) of Mulchaey et al. (2003). In constructing the composite LF we restricted our selection to clusters with $z \leq 0.25$ in order to sample well below the predicted M^*, and used therefore 97 clusters out of 130 systems in the catalog.

The optical photometric data are taken from the SDSS DR2 (York et al. 2000; Stoughton et al. 2002; and Abazajian et al. 2004). The SDSS consists of an imaging survey of π steradians of the northern sky in the five passbands u, g, r, i, z, in the entire optical range from the atmospheric ultraviolet cutoff in the blue to the sensitivity limit of silicon in the red. The survey was carried out using a 2.5 m telescope, an imaging mosaic camera with 30 CCDs, two fiber-fed spectrographs and a 0.5 m telescope for the photometric calibration. The imaging survey is taken in drift-scan mode. The imaging data are processed with a photometric pipeline (PHOTO) especially written for the SDSS data. For each cluster we defined a photometric galaxy catalog as describe in Sect. 3 of Popesso et al. (2004).

For the analysis in this paper we use only SDSS Model magnitudes. Due to a bug of PHOTO, found during the completion of DR1, the model magnitudes are systematically underestimated by about 0.2–0.3 mag for galaxies brighter then 20th magnitude, and accordingly the measured radii are systematically too large. This problem has been fixed in the SDSS DR2, therefore the model magnitude can be considered a good estimate of the galaxy total luminosity at any magnitude and are not dependent on the seeing as the Petrosian magnitudes. Figures 1 and 2 show the difference in the quality of the galaxy photometry between the DR1 and the DR2 data. For this study we only use the revised DR2 for the complete cluster sample.

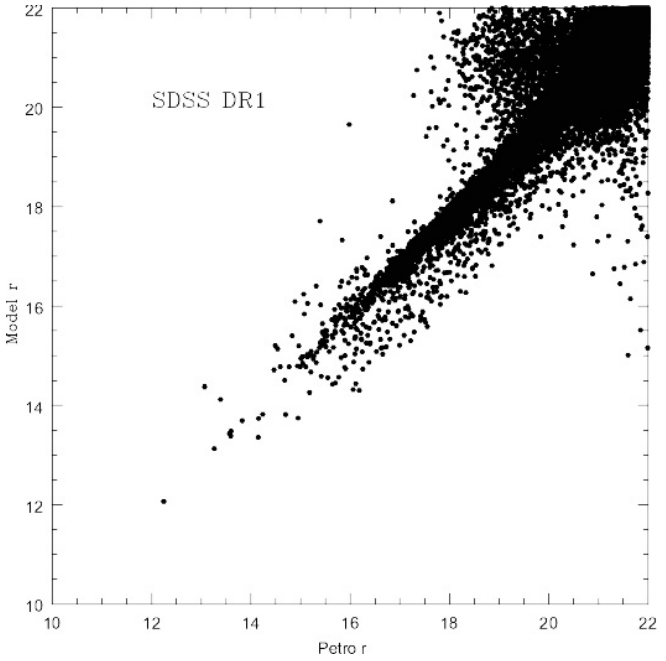

Fig. 1. Petrosian magnitude versus Model magnitude in the Data Release 1 (DR1).

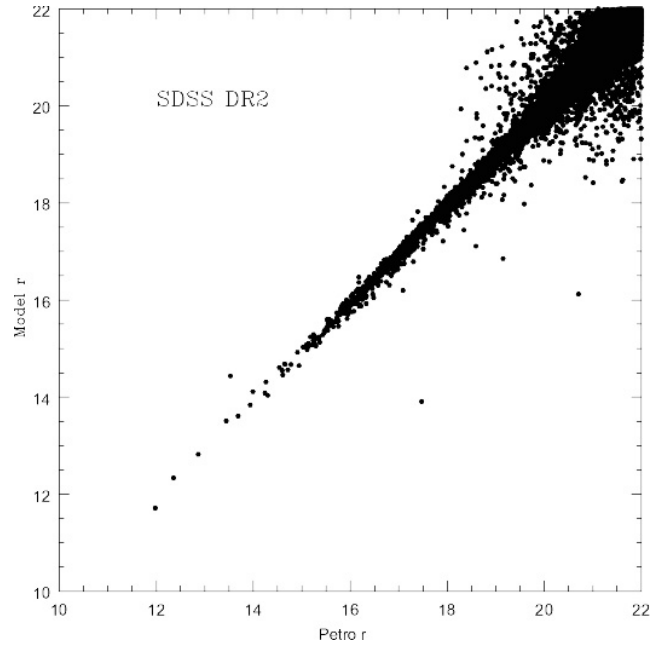

Fig. 2. Petrosian magnitude versus Model magnitude in the Data Release 2 (DR2).

3. The individual luminosity functions

3.1. Background subtraction

We consider two different approaches to the statistical subtraction of the galaxy background. First we calculate a local background in an annulus with inner radius of 3 Mpc h^{-1} from the X-ray cluster center and width of 0.5 deg. The annulus is divided in 20 sectors (Popesso et al. 2004) and those featuring a larger than 3σ deviation from the median galaxy density are discarded from further calculations. In this way other clusters close to the target or voids are not included in the background correction. We compute the galaxies number counts $N^{\rm l}_{\rm bg}(m)\mathrm{d}m$ per bin of magnitude (with a bin width of 0.5 mag) and per squared degree in the remaining area of the annulus. The statistical source of error in this approach is the Poissonian uncertainty of the counts, given by $\sqrt{N^{\rm l}_{\rm bg}(m)}$.

As a second method we derive a global background correction. The galaxy number counts $N^{\rm g}_{\rm bg}(m)\mathrm{d}m$ is derived from the mean of the magnitude number counts determined in five different SDSS sky regions, each with an area of 30 deg^2. The source of uncertainty in this second case is systematic and originates from the presence of large-scale clustering within the galaxy sample, while the Poissonian error of the galaxy counts is small due to the large area involved. We estimate this error as the standard deviation of the mean global number counts, $\sigma^{\rm g}_{\rm bg}(m)$, in the comparison of the five areas. To take into account this systematic source of error also for the the local background, we estimate the background number counts error as $\sigma_{\rm bg}(m) = \max(\sqrt{N^{\rm l}_{\rm bg}(m)}, \sigma^{\rm g}_{\rm bg}(m))$ (Lumdsen et al. 1997) for all the derived quanties. For a detailed comparison of the results of the local and global background estimates see Popesso et al. (2004).

3.2. Luminosity function

We derive the individual cluster luminosity function by subtracting from the galaxy counts measured in a certain region

the local or the global field counts rescaled to the cluster area. We calculate the individual cluster LF within different radii, from 0.3 to 2 Mpc h^{-1}, to study possible dependences of the LF on the clustercentric distance and thus on the density. Following previous works, we exclude from the individual cluster LFs the Brightest Cluster Galaxies (BCG).

To build the Composite LF we transform the apparent magnitude in absolute magnitude according to:

$$M = m - 25 - 5\log_{10}(D_L/1\ \mathrm{Mpc}) - A - K(z) \quad (1)$$

where D_L is the luminosity distance, A is the Galactic extinction and $K(z)$ is the K-correction. We deredden the Petrosian and model magnitudes of galaxies using the Galactic map of Schlegel et al. (1998) in each photometric band. We use the K-correction supplied by Fukugita et al. (1995) for elliptical galaxies, assuming that the main population of our clusters are the old elliptical galaxies at the cluster redshift.

Due to the high accuracy of the SDSS multi-color photometry, the quality of the individual cluster LF is very high. Therefore, to compare the Schechter parameters of the individual LF with those of the composite luminosity function, we fit a Schechter luminosity function to the single clusters by using the fitting method described in the Sect. 4 of Popesso et al. (2004).

4. The composite luminosity function

The composite LF is not only a good method to calculate with high accuracy the cluster LF when the quality of the individual cluster LFs is too low, but it is also a tool to check for the LF universality. The composite LF can be easily interpreted as a mean cluster LF. Therefore, if the LF is universal in all the cluster environments, the distribution of the individual LF parameters should be Gaussian around the corresponding value of the Composite LF parameters. A good description of the calculation of the composite LF can be found in Colless (1989). Following these prescriptions, the Composite LF is built by summing the cluster galaxies in absolute magnitude bins and scaling by the richness of their parent clusters:

$$N_{\mathrm{c}j} = \frac{N_{\mathrm{c}0}}{m_j}\sum_i \frac{N_{ij}}{N_{i0}} \quad (2)$$

where $N_{\mathrm{c}j}$ is the number of galaxies in the jth absolute magnitude bin of the composite LF, N_{ij} is the number in the jth bin of the ith cluster LF, N_{i0} is the normalization used for the ith cluster LF, m_j is the number of clusters contributing to the jth bin and $N_{\mathrm{c}0}$ is the sum of all the normalizations:

$$N_{\mathrm{c}0} = \sum_i N_{i0}. \quad (3)$$

Since all the systems in the cluster sample cover the magnitude region $M \leq -19$ in the five wavebands, we choose that region for the normalization according to the treatment in the literature.

The formal error in the $N_{\mathrm{c}j}$ is computed according to:

$$\delta N_{\mathrm{c}j} = \frac{N_{\mathrm{c}0}}{m_j}\left[\sum_i \left(\frac{\delta N_{ij}}{N_{i0}}\right)^2\right]^{(1/2)} \quad (4)$$

where the $\delta N_{\mathrm{c}j}$ and δN_{ij} are the formal errors in the jth bin of the Composite LF and of the ith cluster LF. Since the ith cluster LF bin is given by the galaxy counts corrected by the field subtraction, the formal error δN_{ij} is calculated as the quadratic sum of the Poissonian error in the counts and the background error.

It is easy to note that in the Colless (1989) prescriptions the jth bin of the Composite LF represents just the mean fraction of galaxies, with respect to the normalization region, of all the clusters contributing to the jth bin.

There are three caveats in the use of the Colless method described above. Firstly, the magnitude limit of all the clusters has to be at least fainter than the limit of the region of normalization ($M < -19$ mag in our case). Secondly, the normalization region has to be large enough to be representative of the richness of the cluster and, thirdly, that the number of clusters contributing to each bin of magnitude has to be statistically significant. If these requirements are satisfied, the Colless (1989) prescriptions can be used to build a Composite LF which extends to the faintest magnitude limit of the cluster sample, with an efficient use of the available data. Therefore, we use the whole magnitude range available with our cluster sample and we include in the Composite LF all the bins with at least 10 contributing clusters.

An alternative method has been recently proposed by Garilli et al. (1999):

$$N_{\mathrm{c}j} = \frac{1}{m_j}\sum_i N_{ij} w_i^{-1} \quad (5)$$

where $N_{\mathrm{c}j}$ and N_{ij} have the same meaning as in the former case, while m_j is the number of clusters with the limiting magnitude deeper than the jth bin and w_i is the weight of each cluster, given by the ratio of the number of galaxies of the ith cluster to the number of galaxies brighter than its magnitude limit in all clusters with fainter magnitude limits (Andreon private communication). The formal error in the Composite LF is computed as:

$$\delta N_{\mathrm{c}j} = \frac{1}{m_j}\sqrt{\sum_i N_{ij} w_i^{-2}}. \quad (6)$$

The important difference of the latter method with regard to the Colless (1989) prescriptions is that the Composite LF is not a simple mean of the galaxy fraction in each bin (multiplied by a normalization constant), but a weighted mean of the cluster galaxy number in each bin of magnitude.

5. Results

Figure 3 shows the Composite LF obtained with the Colless (1989) prescription with a global and local background corrections. In both cases, the Composite LF shows a clear bimodal behavior, showing the upturn of the dwarf galaxies in the magnitude region $-18 \leq M \leq -16$, depending on the waveband. We apply two different approaches in fitting the Composite LF. We divide the Composite LF in two components, a "brigh-end" and a "faint-end" Composite LF, locating by eye the upturn of the dwarf galaxies. We, then, fit the two components separately

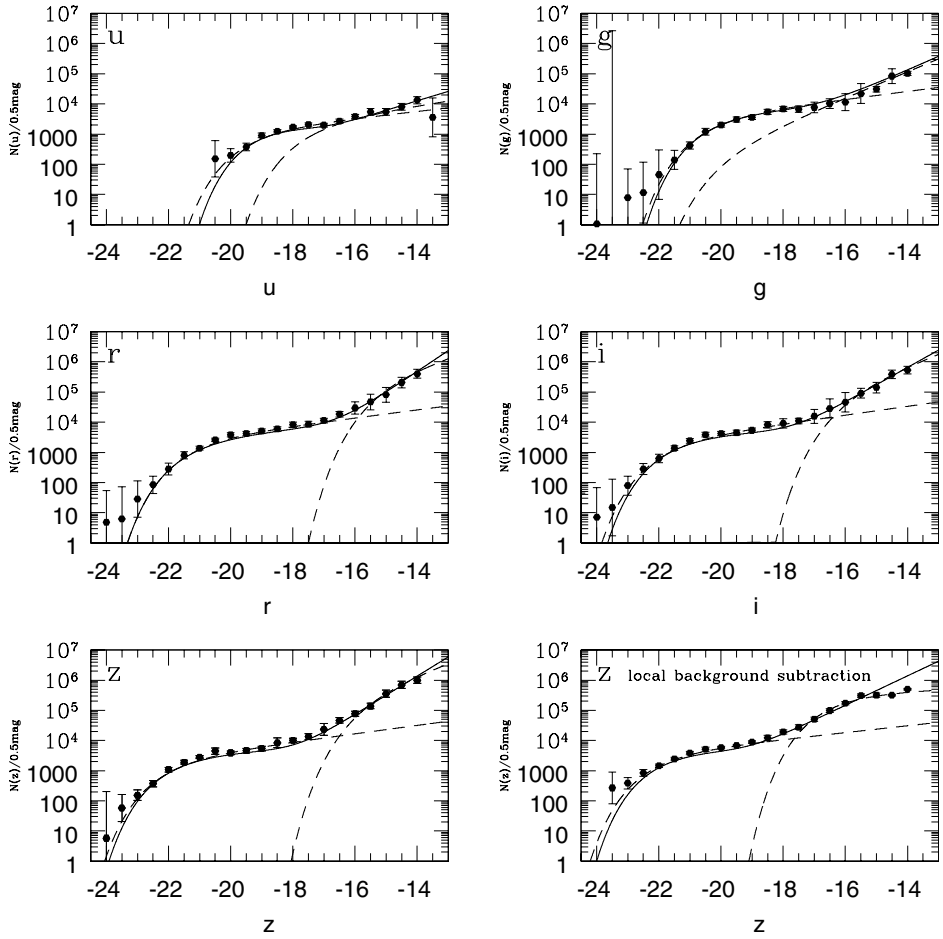

Fig. 3. The Composite LF in the five Sloan bands calculated within 1 Mpc h^{-1} aperture and with a global background correction. For comparison we show also the composite LF in the z band calculated with a local background subtraction. The solid line in each plot is the result of the two Schechter components fit (2Scf), while the dashed line are obtained with the single Schechter component fit (SScf) at the bright and at the faint end of the LF. The 2Scf fit perfectly reproduces the sum of the two single bright and faint components.

using a Single Schechter component fit (SScf). As a second approach, we fit the whole available range of magnitude of the Composite LF with the sum of the two Schechter components (2 Schechter components fit, 2Scf). The dashed lines in Fig. 3 are the results of the SScf method, while the solid line is the fit resulting from the 2Scf procedure. There is a very good agreement between the results of the methods applied. Table 2 lists the values of the Schechter parameters of the bright and the faint LF components obtained with different fitting procedures. The Composite LFs are calculated using different background subtractions and within different cluster radii (from 0.5 to 2.0 Mpc h^{-1}). Figure 4 shows the individual cluster LFs for a subsample of 25 systems of the RASS-SDSS galaxy cluster catalog. We overplotted the results of the SScf method applied to the corresponding Composite LF.

For comparison we also applied the method proposed by Garilli et al. (1999). The plot on the left side in Fig. 5 shows the results obtained applying that method. It is clear that the upturn in the faint magnitude region has disappeared completely and the composite LF is well fitted by a single Schechter function. The results obtained with the Garilli et al. (1999) prescription do not agree within the errors with the results obtained with the Colless method, and show a much flatter LF with a fainter M^* in all the wavebands. Instead, there is a very good agreement (1σ) with the Schechter parameters obtained by Garilli et al. (1999) and Paolillo et al. (2001), who applied the same method to derive the composite LF. The Composite LF obtained with this prescription is not a good representation of the mean cluster LF since it does not reproduce the features visible in the individual cluster LFs (see Fig. 4). The reason of the disagreement between the Composite LF obtained with the Garilli's method and the individual LFs is due to the different weighting method applied by Garilli et al. (1999). As shown in the plot on the right side of Fig. 5, the weight in the Garilli et al. (1999) method depends strongly on the cluster magnitude limits. The weight w_i^{-1} is a decreasing function of the cluster $M_{\rm lim}$, therefore, the clusters with fainter $M_{\rm lim}$, which contribute to the faint magnitude bins, are heavily down-weighted. This bias explains the lack of the dwarf upturn in the Composite LF.

In the following analysis we consider only the results obtained with the Colless (1989) prescription.

5.1. The bright end

The Schechter parameters α and M^* obtained for the Composite LF derived with the Colless (1989) prescriptions

Table 2. Schechter parameters of the Composite LF.

	u		g		r		i		z	
r	α_u	M^*_u	α_g	M^*_g	α_r	M^*_r	α_i	M^*_i	α_z	M^*_z
SScf – Bright component, global background subtraction										
0.5	-1.31 ± 0.16	-19.59 ± 0.85	-1.18 ± 0.05	-20.52 ± 0.26	-1.29 ± 0.09	-21.54 ± 0.39	-1.20 ± 0.06	-21.77 ± 0.30	-1.23 ± 0.07	-22.09 ± 0.30
1.0	-1.15 ± 0.15	-19.11 ± 0.48	-1.19 ± 0.04	-20.39 ± 0.15	-1.30 ± 0.06	-21.35 ± 0.19	-1.07 ± 0.08	-21.62 ± 0.15	-1.16 ± 0.06	-21.86 ± 0.18
1.5	-1.16 ± 0.14	-18.92 ± 0.39	-1.33 ± 0.04	-20.59 ± 0.20	-1.33 ± 0.06	-21.57 ± 0.21	-1.22 ± 0.06	-21.76 ± 0.17	-1.28 ± 0.06	-22.04 ± 0.25
2.0	-1.39 ± 0.13	-19.44 ± 0.61	-1.44 ± 0.04	-20.83 ± 0.22	-1.34 ± 0.07	-21.63 ± 0.22	-1.25 ± 0.06	-22.19 ± 0.25	-1.25 ± 0.07	-22.11 ± 0.22
SScf – Bright component, local background subtraction										
0.5	-1.28 ± 0.15	-19.38 ± 0.63	-1.25 ± 0.04	-20.64 ± 0.23	-1.41 ± 0.07	-21.81 ± 0.43	-1.33 ± 0.05	-22.13 ± 0.33	-1.33 ± 0.05	-22.44 ± 0.27
1.0	-1.34 ± 0.08	-18.93 ± 0.18	-1.44 ± 0.05	-20.76 ± 0.19	-1.33 ± 0.06	-21.40 ± 0.20	-1.25 ± 0.06	-21.63 ± 0.16	-1.28 ± 0.06	-21.99 ± 0.18
1.5	-1.37 ± 0.17	-19.30 ± 1.03	-1.24 ± 0.10	-20.49 ± 0.19	-1.40 ± 0.05	-21.71 ± 0.19	-1.47 ± 0.04	-22.14 ± 0.18	-1.35 ± 0.06	-22.07 ± 0.16
2.0	-1.38 ± 0.10	-19.40 ± 0.71	-1.02 ± 0.16	-20.35 ± 0.21	-1.51 ± 0.06	-21.93 ± 0.24	-1.54 ± 0.03	-22.31 ± 0.16	-1.51 ± 0.05	-22.46 ± 0.19
SScf – Faint component, global background subtraction						SScf – Faint component, local background subtraction				
r	α_u	α_g	α_r	α_i	α_z	α_u	α_g	α_r	α_i	α_z
0.5	-1.50 ± 0.35	-1.98 ± 0.38	-1.96 ± 0.24	-1.81 ± 0.15	-1.80 ± 0.16	-1.60 ± 0.25	-2.16 ± 0.09	-2.18 ± 0.04	-1.98 ± 0.08	-2.18 ± 0.03
1.0	-1.40 ± 0.14	-1.88 ± 0.24	-1.54 ± 0.50	-1.61 ± 0.08	-2.24 ± 0.10	-1.50 ± 0.33	-2.45 ± 0.47	-1.83 ± 0.06	-2.27 ± 0.07	-1.72 ± 0.05
1.5	-1.69 ± 0.07	-1.73 ± 0.25	-2.11 ± 0.37	-1.74 ± 0.21	-2.27 ± 0.05	-1.73 ± 0.03	-1.73 ± 0.05	-1.53 ± 0.07	-1.90 ± 0.07	-1.78 ± 0.05
2.0	-1.53 ± 0.06	-2.05 ± 0.20	-1.74 ± 0.11	-2.09 ± 0.11	-2.44 ± 0.11	-1.66 ± 0.03	-1.64 ± 0.13	-2.08 ± 0.06	-1.91 ± 0.05	-2.35 ± 0.02
2Scf – Bright component, global background subtraction										
0.5	-0.92 ± 0.13	-18.00 ± 0.50	-1.30 ± 0.13	-20.75 ± 0.46	-1.30 ± 0.12	-21.50 ± 0.51	-1.09 ± 0.13	-21.54 ± 0.41	-1.23 ± 0.11	-22.19 ± 0.44
1.0	-1.59 ± 0.13	-19.24 ± 0.53	-0.55 ± 0.17	-19.67 ± 0.20	-1.03 ± 0.13	-20.90 ± 0.26	-1.14 ± 0.11	-21.56 ± 0.26	-1.07 ± 0.12	-21.73 ± 0.27
1.5	-1.27 ± 0.22	-19.40 ± 0.23	-1.41 ± 0.16	-20.80 ± 0.46	-1.39 ± 0.07	-21.50 ± 0.23	-1.20 ± 0.04	-21.98 ± 0.26	-1.06 ± 0.16	-21.69 ± 0.38
2.0	-1.50 ± 0.17	-20.59 ± 0.09	-1.58 ± 0.15	-21.53 ± 0.82	-1.06 ± 0.10	-21.24 ± 0.37	-0.94 ± 0.22	-21.61 ± 0.49	-1.29 ± 0.03	-22.17 ± 0.36
2Scf – Bright component, local background subtraction										
0.5	-0.68 ± 0.18	-18.32 ± 0.33	-1.24 ± 0.16	-20.62 ± 0.46	-1.23 ± 0.19	-21.36 ± 0.60	-1.16 ± 0.19	-21.79 ± 0.62	-1.22 ± 0.12	-22.14 ± 0.44
1.0	-0.95 ± 0.23	-19.53 ± 0.30	-1.23 ± 0.11	-20.39 ± 0.27	-1.05 ± 0.13	-20.95 ± 0.27	-1.17 ± 0.13	-21.64 ± 0.29	-1.06 ± 0.12	-21.70 ± 0.26
1.5	-1.71 ± 0.13	-20.36 ± 0.26	-0.91 ± 0.28	-20.23 ± 0.34	-0.76 ± 0.13	-20.86 ± 0.20	-1.11 ± 0.09	-21.51 ± 0.21	-1.02 ± 0.12	-21.71 ± 0.21
2.0	-0.96 ± 0.49	-18.75 ± 0.76	-0.99 ± 0.23	-20.15 ± 0.35	-1.03 ± 0.14	-21.19 ± 0.23	-1.27 ± 0.11	-21.82 ± 0.26	-1.46 ± 0.06	-22.41 ± 0.26
2Scf – Faint component, global background subtraction										
0.5	-0.88 ± 0.18	-18.92 ± 0.45	-2.44 ± 0.25	-16.99 ± 0.31	-2.38 ± 0.15	-17.76 ± 0.23	-2.09 ± 0.07	-18.34 ± 0.19	-2.28 ± 0.08	-18.59 ± 0.21
1.0	0.00 ± 0.00	-18.09 ± 0.37	-2.04 ± 0.03	-17.89 ± 0.11	-2.01 ± 0.05	-18.40 ± 0.15	-2.36 ± 0.05	-18.86 ± 0.16	-2.22 ± 0.06	-19.09 ± 0.17
1.5	-2.65 ± 0.90	-15.43 ± 0.44	-2.54 ± 0.18	-17.18 ± 0.25	-2.79 ± 0.14	-17.40 ± 0.18	-2.83 ± 0.07	-18.00 ± 0.14	-2.70 ± 0.07	-18.71 ± 0.12
2.0	0.00 ± 0.05	-17.31 ± 0.01	-2.52 ± 0.30	-17.52 ± 0.57	-2.03 ± 0.08	-18.63 ± 0.21	-2.21 ± 0.08	-18.91 ± 0.23	-2.76 ± 0.05	-18.64 ± 0.14
2Scf – Faint component,local background subtraction										
0.5	0.00 ± 0.00	-15.63 ± 0.26	-2.23 ± 0.25	-17.26 ± 0.32	-2.18 ± 0.18	-18.12 ± 0.26	-2.17 ± 0.19	-18.51 ± 0.22	-2.34 ± 0.12	-18.57 ± 0.20
1.0	-1.64 ± 0.25	-19.79 ± 4.04	-2.84 ± 0.13	-17.27 ± 0.13	-2.02 ± 0.05	-18.42 ± 0.15	-2.45 ± 0.13	-18.96 ± 0.17	-2.21 ± 0.06	-19.08 ± 0.16
1.5	-0.76 ± 5.46	-18.71 ± 0.87	-1.86 ± 0.07	-18.49 ± 0.26	-1.92 ± 0.03	-18.94 ± 0.13	-2.13 ± 0.03	-19.07 ± 0.13	-2.25 ± 0.05	-19.45 ± 0.13
2.0	-1.62 ± 0.04	-18.71 ± 2.17	-2.26 ± 0.07	-18.26 ± 0.18	-2.22 ± 0.04	-19.06 ± 0.15	-2.54 ± 0.10	-19.21 ± 0.14	-2.61 ± 0.06	-19.16 ± 0.12

The Schechter parameters of the bright and the faint end of the composite LF. The results are obtained with a single Schechter component fit (SScf) and with a two Schechter components fit (2Scf). For each case the fit procedure was applied to the composite LF calculated within 4 different clustercentric distances, 0.5, 1.0, 1.5 and 2.0 Mpc h^{-1} and with different background corrections.

with the local and global background corrections agree very well at any radius (in the worse cases within 1.5σ). There is also a very good agreement within the errors for M^* obtained with different fitting procedures. The slope of the bright component calculated with the SScf method is systematically steeper than the slope obtained with the 2Scf procedure. This is due to the fact that in the 2Scf method the fitting function is the sum of two components. Consequently, the slope of the bright component does not represent only the bright galaxies population but depends also on the slope and M^* of the second (faint) component. Therefore, in the following analysis we consider the parameters of the bright component obtained with the SScf method as representative of the bright galaxies population in clusters.

Figure 6 shows the error contours of these Schechter parameters calculated for the Composite LFs measured within 3 different cluster radii, 1.0, 1.5 and 2.0 Mpc h^{-1} in the case of a global background correction. α and M^* do not seem to depend on the clustercentric distance since the error contours overlap in all wavebands, except for the g band. However, the behavior of the Schechter parameters in this band is not confirmed by the same Composite LF calculated with the local background subtraction. Therefore, we can conclude that there is no significant difference in the bright end LF measured in different aperture radii.

To check the universality of the cluster LF, we compare the Schechter parameters of the bright component of Composite LF with the Schechter parameters derived by fitting the individual cluster LFs. Figure 7 shows the distributions of M^* and α of the individual cluster LFs derived in the z band within 1 Mpc h^{-1} from the cluster center and with a global background correction. The vertical dashed lines in the plots show the value of the corresponding Composite LF parameter and the 3σ error interval. The plots a and b in the Fig. 7 show the distributions of M^* and α when a single Schechter luminosity function is fitted to the galaxies in the whole available magnitude range of each cluster (including the dwarf region). It is clear from those distributions that the "bright end" Composite LF is not a good representation of the mean behavior of the individual LFs: the individual LFs seems to be systematically steeper and the dispersion of M^* is larger than 2 mag. The distributions of both parameters change drastically if the galaxies in the dwarfs region are excluded from the fits. Plots c and d of the Fig. 7 clearly show that the distributions become in both cases close to

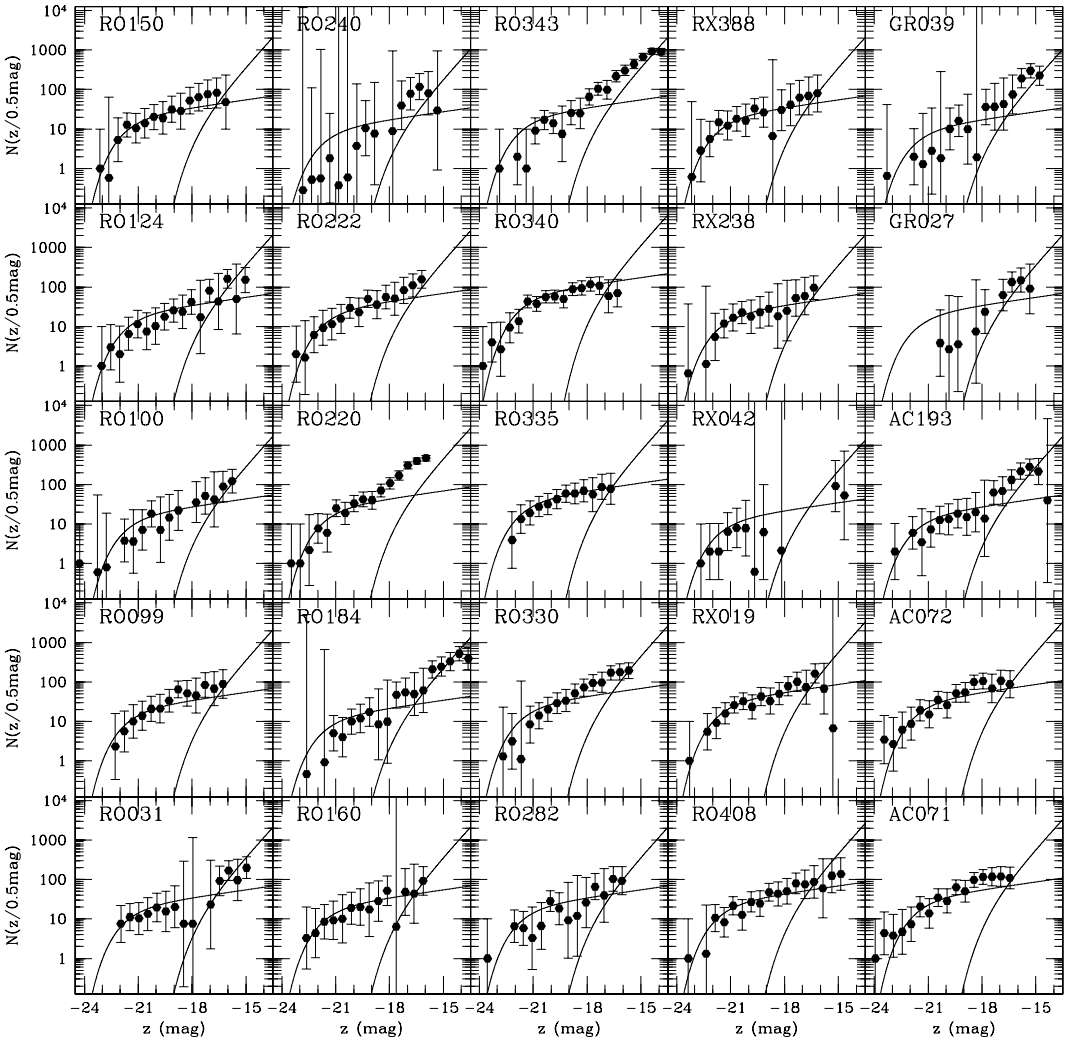

Fig. 4. The individual cluster luminosity functions for 25 clusters of the RASS-SDSS galaxy cluster catalog, calculated within 1 Mpc h^{-1} aperture and with a global background subtraction. The solid line in the plots are the results of the SSfc method applied to the corresponding Composite LF. The upturn of the dwarf and the steepening of the LFs at the faint end is evident in several clusters.

a Gaussian with the maximum coincident with the value of the corresponding Composite LF parameter. The dispersion of the distribution of α seems to be larger than the 3σ error interval of the Composite LF parameter. Therefore, we conclude that the Composite LF is a very good representation of the mean behavior of the individual cluster "bright end" LFs, but it is not universal. Nevertheless, we assume that the dwarf upturn of all the clusters in the sample has the same location observed in the Composite LF ($M_z \sim -18$). A brighter upturn could give a steeper individual LF and, therefore, it could explain the excess of clusters in the region $\alpha \leq -1.3$ in the plot *d* of Fig. 7.

5.2. The faint end

The results obtained for the fits of the faint LF components with different fitting procedures, background corrections and cluster apertures are listed in Table 2. For the SScf method we report only the slope of the faint-end component in each band and not the values of M^*. In fact, the faint end of the composite LF does not contain a sufficient number of points to constrain in a meaningful way the characteristic magnitude, and the statistical errors of M^* are larger than 1 mag. We listed in the same table α and M^* measured with the 2Scf method. In this case the characteristic magnitude of the faint end is constrained by the slope of the bright component.

As Table 3 shows, the "faint end" Composite LF is much steeper than the "bright end" LF at any radius and in any passband with both fitting procedures. There is a discrepancy between the values of the slope of the SScf and the 2Scf methods in all the analysed cases. The reason of the disagreement is the same observed for the slopes of the bright component. The mean value of α derived with the SScf method in the case of a global background correction is 1.60 in u, 1.84 in g, 1.81 in r, 1.76 in i and 2.07 in z. The slope do not show a dependence on the waveband and on the distance from the cluster center. The result is confirmed also by the values given by the 2Scf procedure.

Valotto et al. (2001) use a numerical simulation of a hierarchical universe to show that many "clusters" identified from two dimensional galaxy distributions might result principally

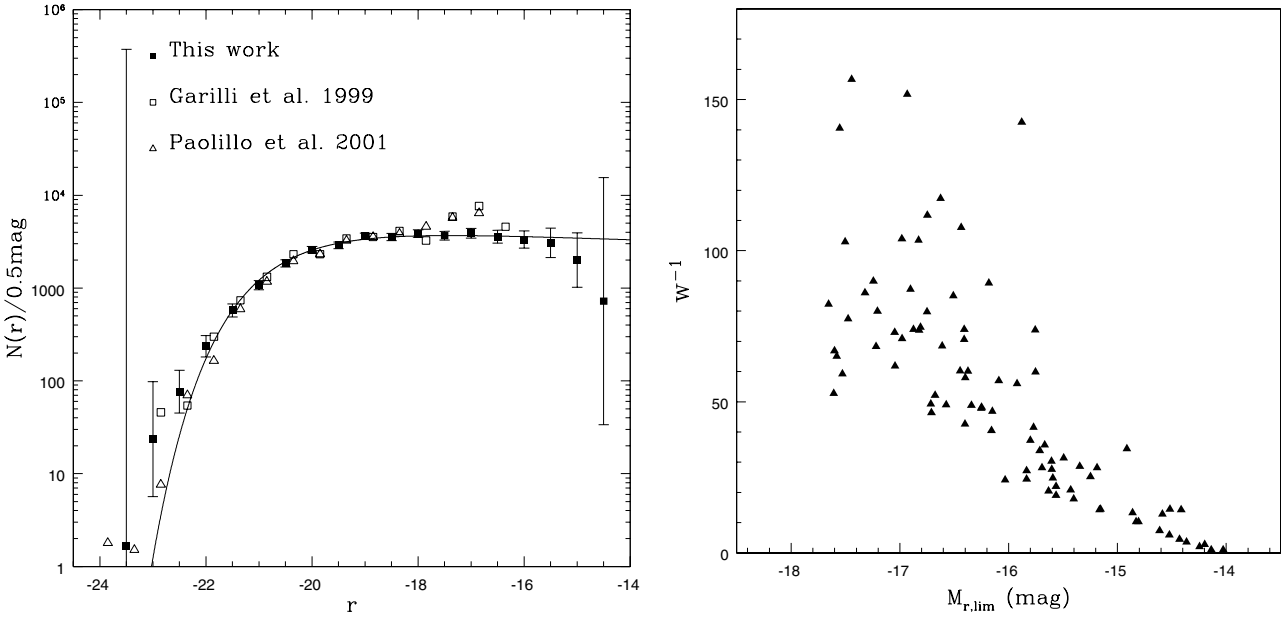

Fig. 5. The results obtained applying the Garilli et al. (1999) method. The plot on the left side shows the Composite LF in the r Sloan band (filled squares). For comparison we plot also the Composite LF obtained by Garilli et al. (1999) (empty squares) and by Paolillo et al. (2001) (empty triangles). The three LFs agree very well (within 1σ) in the characteristic magnitude and in the faint end slope. However the Composite cluster LFs obtained with this prescription do not reproduce the main features observed in the individual cluster LFs (see Fig. 4). The reason for the disagreement is the weighing method in the Garilli's prescription. The plot on the right side shows the dependence of the weight w_i on the magnitude limit of the single cluster. The systems with very faint $M_{\rm lim}$, which contribute to the faint magnitude bins in the composite LF, are heavily down-weighted. The bias explains the lack of the upturn in the dwarf magnitude range observed in the individual cluster LFs.

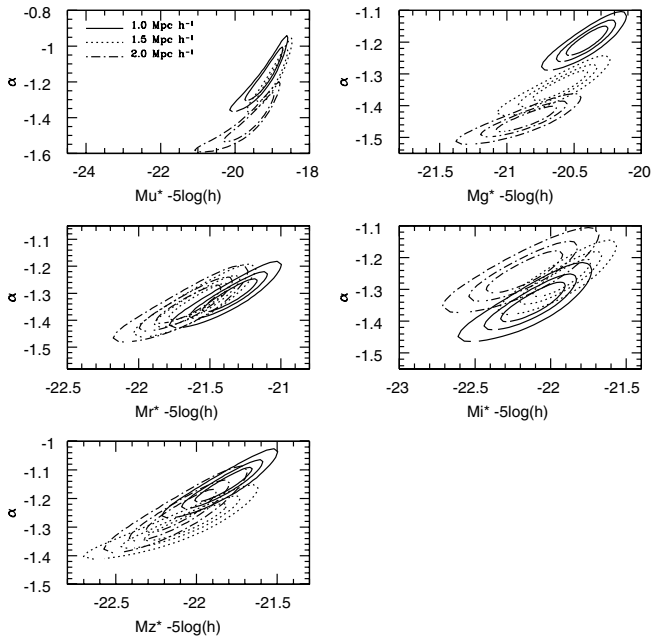

Fig. 6. 1, 2 and 3σ contours of the best fit Schechter parameters for the bright component of the Composite LF. The contours are derived with the SScf method applied to the bright end of the Composite LF. The LF is calculated with a global background subtraction within 1, 1.5 and 2 Mpc h^{-1} apertures.

from the projection of a large-scale structure alone the line of sight. They suggest that attempts to derive the LF for these "clusters" using the standard background subtraction procedure lead to deriving an LF with a steep faint-end slope, despite the fact that the actual input LF had a flat faint-end. Since the RASS-SDSS galaxy cluster sample comprises only clusters detected in X-rays, all the systems contributing to the "faint-end" Composite LF (26 clusters with $M_{z\rm lim} \geq -16$) are not a projection effect but are real clusters. Moreover, the use of a local background subtraction, which takes into account the presence of large-scale structure, confirms the steepening of the Composite LF observed with the global background subtraction. Valotto et al. (2004) compare the composite luminosity function of a optically selected sample of clusters with an X-ray selected sample of systems from the RASS1 bright clusters catalog of De Grandi et al. (1999). They show that the composite LF of the former sample presents a steep faint end due to projection effects, while the composite LF of the X-ray selected sample is flat with a slope of –1.1 in the magnitude range $M_{\rm b_J} \leq -16.5$. Our results are still in agreement with Valotto et al. (2004), since we are observing a much fainter population with $-16 \leq M_{\rm g} - 5\log(h) \leq -14$. Nevertheless, one could still suspect that the observed steepening of the faint end in the individual clusters is due to a baclground object at higher redshift and the same line of sight. In fact, in this case, both the global and local background corrections would fail to subtract this contribution. To test this possibility, we use the SDSS spectroscopic redshifts to check the presence of galaxy overdensities at higher redshift and in the same line of sight of the systems of interest. Only RO184 shows a second object in background while all the others clusters with and without

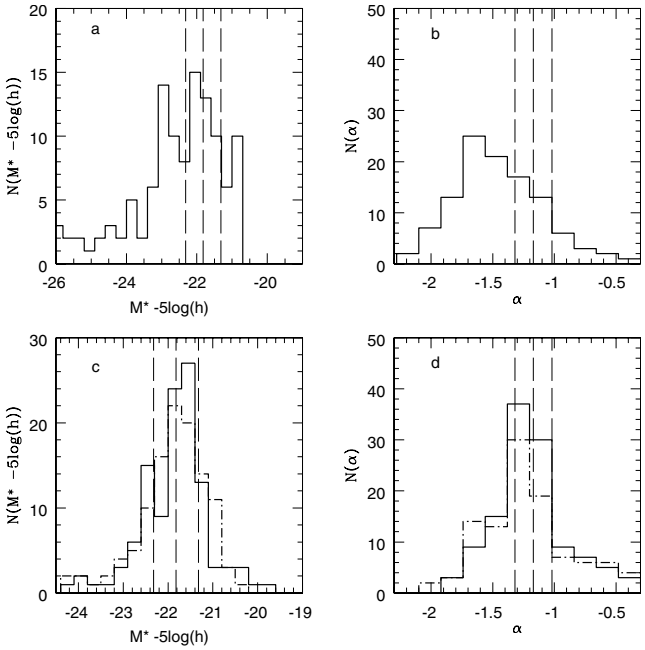

Fig. 7. Distribution of the Schechter parameters α and M^* of the individual cluster LFs in the sample, calculated in the z band within 1 Mpc h^{-1} and with a global background correction. Plots a and b show the distribution of M^* α, respectively, obtained by fitting a single Schechter luminosity function to the galaxies in the whole available magnitude range of each cluster. Plots c and d show the distribution of M^* and α , respectively, obtained by fitting a single Schechter luminosity function to the galaxies brighter than the magnitude of the dwarf upturn $M_Z \leq -18$. The dashed lines in plots c and d are the distributions obtained from the fits with α and M^* being free parameters. The solid line in plots c is the distribution of M^* when α is fixed to the value of the corresponding bright component of the Composite LF calculated with the SScf method. The solid line in plot d is the distribution of α when M^* is fixed to the value of the Composite LF. The vertical dashed lines in each plots indicate the value of the corresponding parameters of the bright component in the Composite LF and its 3σ error interval.

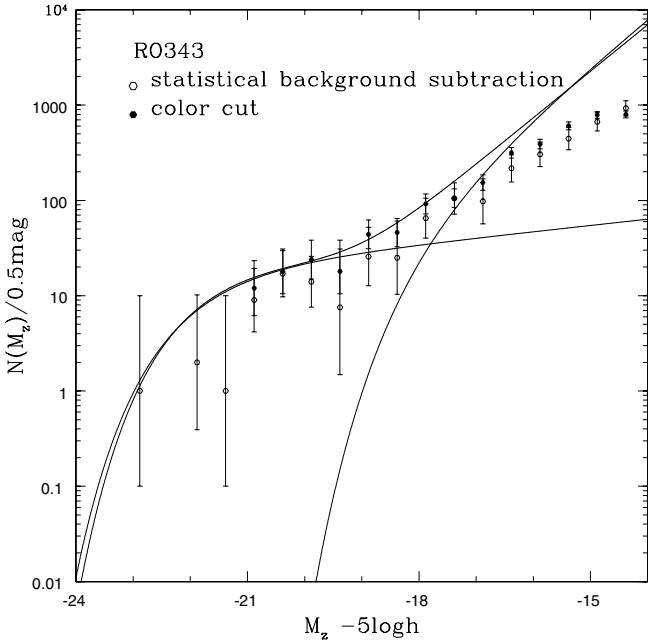

Fig. 8. The two different methods of background subtraction. The cluster RO343 is one of the clusters showing a significant steepening of the LF in the faint magnitude range. The filled points indicate the cluster LF obtained with a cut in the $g - r - r - i$ plane (Garilli et al. 1999). The empty points are the LF obtained with the statistical local background correction applied to obtain the composite LF analysed in the paper. The methods of background subtraction agree perfectly within the errors. The error bars in the color-cut method are the Poissonian error in the galaxy counts. The color cut method excludes all the galaxies redder than the color of an elliptical galaxy at the cluster redshift. Therefore, the steepening in the faint end can not be due to galaxies at higher redshift in a second cluster or in the large scale structure behind the cluster, but should be due to the presence of a real cluster population. A bluer color cut deletes the contribution of the bright elliptical cluster galaxies leaving the faint end LF. This implies that the faint end LF is dominated by late-type galaxies.

steepening in the individual LF present the same single peak redshift distribution.

As an additional test we have measured the individual cluster LF with a color cut method in the same way as Garilli et al. (1999). We use the $g - r$ and $r - i$ galaxy colors defined in Fukugita et al. (1995). We define our color cut in order to exclude all the galaxies redder than the expected color of the ellipticals at the cluster redshift, and the late type galaxies in foreground. We observe that the systems with a significant steepening in the individual LF obtained with a statistical background subtraction show the same feature also with the color cut method (Fig. 8). This implies that we are not observing the contribution of large scale structures but a real cluster faint population. Moreover, we observe that the faint-end of those clusters is due to galaxies with colors compatible with spiral galaxies at the redshift of the cluster. In conclusion, then, the observed steepening of the Composite LF in the considered magnitude range is real.

Even if the Schechter function with the values reported in Table 2 offers a very good fit to the data (reduced $\chi^2 \leq 1.5$ in the worst case), the "faint end" Composite LF contains only few points. Therefore, the slope α has to be considered as a good indicator of the steepening of the LF in this magnitude region, but does not allow a detailed analysis of the behavior of the Composite LF. To study in more detail the behavior of the "fain-end" Composite LF as a function of the waveband and of the distance from the center, we define the Dwarf to Giant Ratio (DGR) in each band as the ratio between the number of galaxies of the "faint end" Composite LF to the number of galaxies of the "bright end" Composite LF. We define DGR as the ratio between the number of galaxies in the magnitude range $-18 \leq M \leq -16.5$ and the number of galaxies brither than –20 mag (except in the u band where we count the galaxies brighter than –19 mag). Figure 9 shows the behavior of DGR in each band as a function of the clustercentric distance. The filled points are derived in the case of a global background subtraction, while the empty points in the case of a local background subtraction. The two results do not agree perfectly on the DGR value, but they reproduce the same dependence on the clustercentric distance. In each waveband the DGR seems to slightly increase from the very center,

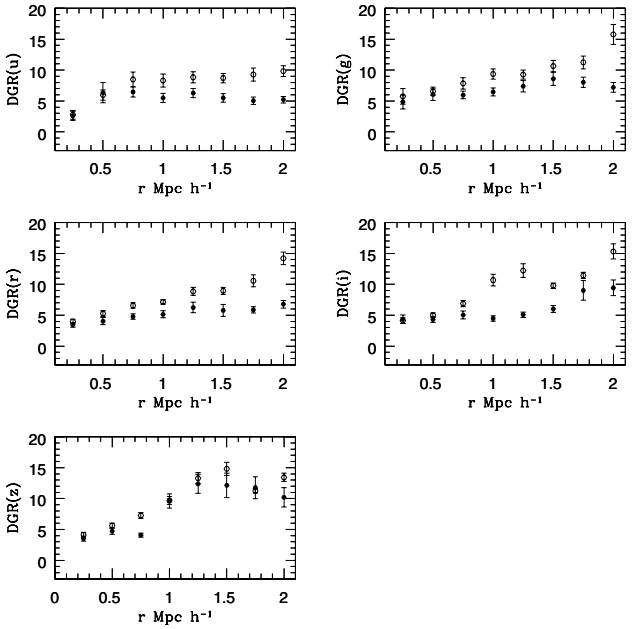

Fig. 9. Dwarf to Giant Ratio (DGR) as a function of the cluster radii in the 5 wavebands. DGR is derived from the Composite LF calculated with a global background correction (filled points) and a local background correction (empty points).

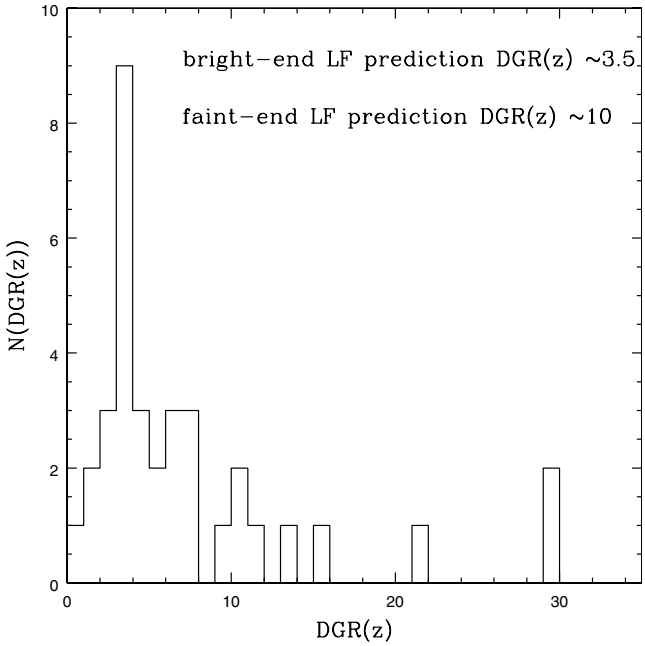

Fig. 10. Distribution of the DGR(z). DGR(z) is defined as as the ratio between the number of galaxies brighter than –20 mag and the number of galaxies in the magnitude range $-18. \leq M_z \leq -16.5$. The faint magnitude range in the definition of DGR(z) is large enough to be representative of the dwarf population while the number of clusters with magnitude limits fainter than –16.5 mag is still large (35 systems) to be statistically significant. The value of DGR(z) predicted by the "bright end" Composite LF (without the dwarf population) is 3.5, while the value predicted with the presence of the "faint-end" Composite LF if around 10.

0.3 Mpc h^{-1}, to 1.0 Mpc h^{-1}. The mean value of DGR increases from the u band (5) to the z band (10).

To test whether the "faint-end" Composite LF is a standard representation of the dwarf population of galaxy clusters or if it is due to the contribution of few particular clusters, we define a DGR for the individual objects and compare it to the DGR of the Composite LF. Figure 10 shows the distribution of the DGR calculated for the single clusters in the z band. The faint magnitude range in the definition of DGR(z) is large enough to be representative of the dwarf population while the number of clusters with magnitude limits fainter than –16.5 mag is still large (35 systems) to be statistically significant. It is important to stress that the value of DGR(z) predicted by the "bright end" Composite LF (without the dwarf population) is 3.5, while the value predicted with the presence of the "faint-end" Composite LF is around 10. As shown in Fig. 10, there is a large spread in the distribution of DGR(z). The histogram in the figure shows a clear peak around the value predicted by the "bright end" LF (3.5), and a large number of objects (1/2) at values larger than this. This result indicates that the behavior of the faint end LF in not universal. We conclude that there seem to exist two different kinds of cluster populations depending on the excess of the dwarf galaxies.

To study the spread of the distribution in DGR(z), we plot DGR(z) versus the cluster richness and versus the M^* of the individual cluster bright-end LF, as shown in Figs. 11 and 12, respectively. We do not find any correlation between the parameters. The Spearman's rank coefficient is very low in both cases and with a probability of non correlation close to 1. However Fig. 13 shows that DGR(z) is significantly anti-correlated with several cluster global properties, i.e. the X-ray and optical luminosities (all the correlations are very significant, 1×10^{-4}–1×10^{-5}, according to a Spearman correlation test). Since L_X correlates with the cluster mass (Reiprich & Böhringer 2001), we conclude that the more massive a cluster, the lower its fraction of dwarf galaxies. The anti-correlation between cluster DGRs and cluster luminosities is most likely due to the choice of a fixed metric aperture for all the clusters. In fact, a fixed metric aperture samples larger (smaller) fractions of the virialized regions of clusters of smaller (respectively, larger) masses, and DGR is known to decrease with cluster-centric distance as showed in Fig. 9 of this section. Therefore, because of this effect, the different cluster physical sizes must be taken into account before comparing different cluster LFs.

In our analysis we do not take into account possible low surface brightness selection effects. Unfortunately, the analysis of the completness limits in surface brightness of the SDSS galaxy photometric sample is not yet completed. Therefore, the luminosity function analysed in this paper should be considered as a lower limit of the true cluster LF, since we could miss low surface brightness galaxies especially at the faint end. Bernstein et al. (1995), Ulmer et al. (1996) and Adami et al. (2000) explore these issues in a series of papers on the faint LF of the Coma cluster and conclude that LSB galaxies in Coma were inconsequential. Moreover, Cross et al. (2004) compare the completeness limits in magnitude and surface brightness of SDSS-EDR and SDSS-DR1 with the Millennium Galaxy Catalogue (MCG). MCG is a deep survey with a limit

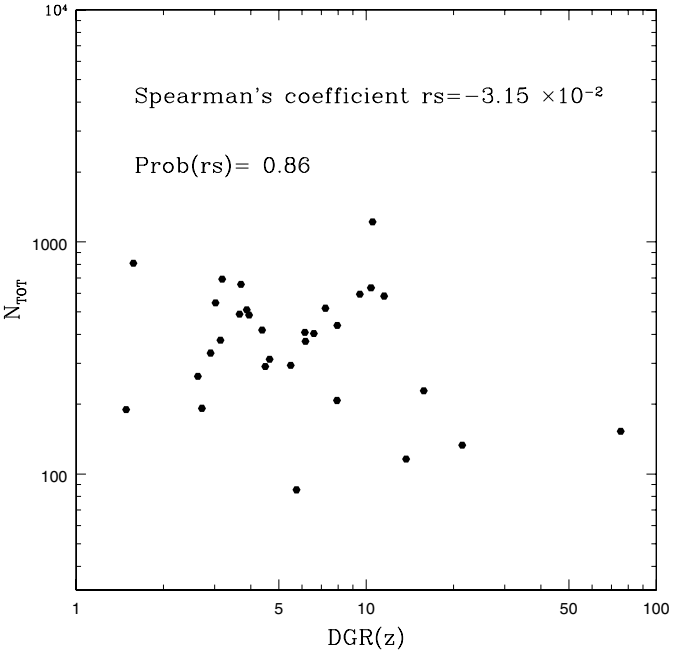

Fig. 11. DGR versus the cluster richness in the z band within 1 Mpc h^{-1} in the case of global background subtraction.

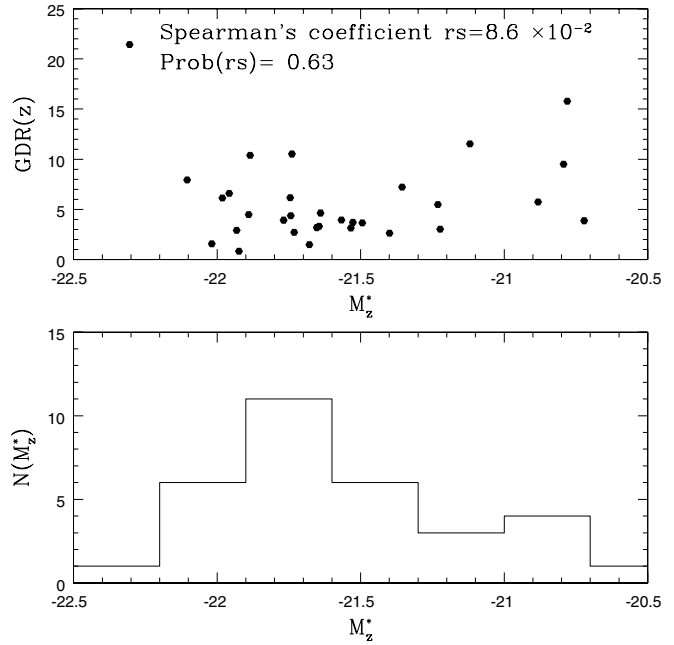

Fig. 12. The upper panel shows DGR versus the characteristic magnitude of the individual bright component LF derived within 1 Mpc h^{-1} in the case of global background subtraction. The bottom panel shows the histogram of M^* for the subsample of clusters. The histogram mimics the behavior of the whole sample showed in the panel c) of Fig. 7.

in surface brightness of 26 mag arcsec^{-2}. They use the MCG bright galaxy catalogue with galaxies in the magnitude range $16 \leq B \leq 20$ (where $B = g + 0.39(g - r) + 0.21$ for DR1 magnitudes) for the comparison with the SDSS-EDR-DR1 catalog. They show that in the range $21 \leq \mu_e \leq 25$ mag arcsec^{-2} the incompleteness of SDSS-EDR is less than 5% and is around 10% in the range $25 \leq \mu_e \leq 26$ mag arcsec^{-2}. In the present work, for most of the clusters the galaxies contributing to the DGR are faint galaxies in the magnitude range $19 \leq r \leq 21$ mag. In this region of magnitudes 65% of the objects lie at $\mu_e \leq 23$ mag arcsec^{-2}, 30% in the range $23 < \mu_e \leq 24$ mag arcsec^{-2}, and 5% at $\mu_e \geq 25$ mag arcsec^{-2}. If we can apply also in this range of magnitude the results of Cross et al. (2004), the incompleteness correction for low surface brightness selection effects should be around 5%. Therefore we expect that the LSB galaxies do not contribute in a egregious way to our luminosity function and cannot change significantly the DGR calculated in the paper.

5.3. Comparison with previous work

The results obtained by previous works are listed in Table 1. All the works in the literature analyse only the relatively bright end of the cluster LF. In Fig. 14 is shown the very good agreement between our results in the g band and the Composite LF of De Propris et al. (2003), who use the 2df spectroscopic data to define the cluster membership. It is clear in the figure that even the 2df composite LF is not enough deep to cover the dwarf galaxy region analysed in this work. Therefore, we can compare only our bright end composite LF with the results found in the literature.

We consider mainly the luminosity function in the g band since there is a large number of b and g band cluster composite LFs in the literature to compare with. After correcting the absolute magnitudes for the different cosmology and for colors, our M^*_g perfectly agrees with almost all the the previous results except for Goto et al. (2002b). The disagreement with this work is larger than 3σ. The reason for the discrepancy with previous work based on SDSS data is ascribable to the different quality of the photometry between the last data release (DR2), used in this work, and the Early Data Release (EDR) used in Goto et al. (2002a).

The slopes of the Composite LF in the g band retrieved from the literature lie in a very large range of values from –1.50 to –0.94. Therefore, there is not an overall agreement in the literature about the slope of the cluster composite LF. Nevertheless, several of the works retrieved in the literature should not be taken into account in this comparison. In fact, the results of Garilli et al. (1999) and Paolillo et al. (2001) should be excluded from our analysis , since we discussed in a previous paragraph that their results depend on the method applied to derive the composite LF. Moreover, we would exclude from our analysis also the results of Goto et al. (2002b) for two different reasons. First, Goto et al. (2002a) use a different SDSS dataset (EDR) with lower quality in the photometry. Secondly, in that work the background is calculated locally in an annulus around the cluster center with outer radius of 1.3 Mpc h^{-1} and inner radius of 1.0 Mpc h^{-1}. Since the background is calculated within the cluster region (within an Abell radius of 1.5 Mpc), where the fraction of cluster galaxies could be very high, such background correction would subtract to a substantial degree the contribution of that cluster galaxy population from the individual and the Composite LF. This suspicious background subtraction could explain the very flat LF obtained by

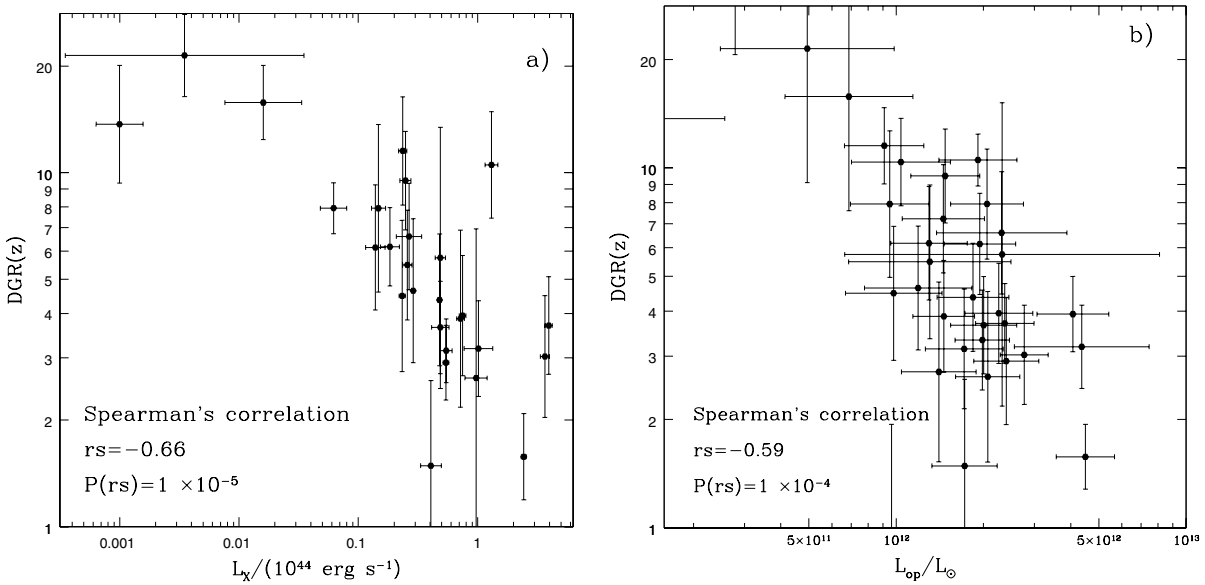

Fig. 13. The correlation between DGR(z) and the X-ray (panel **a)** and optical (panel **b**)) luminosities. DGR(z) clearly anticorrelates with the cluster luminosities as confirmed by a Spearman's test. Since DGR(z) increases with the clustercentric distance as confirmed in the previous sections, the anti-correlation between cluster DGRs and cluster luminosities is most likely due to the choice of a fixed metric aperture for all the clusters.

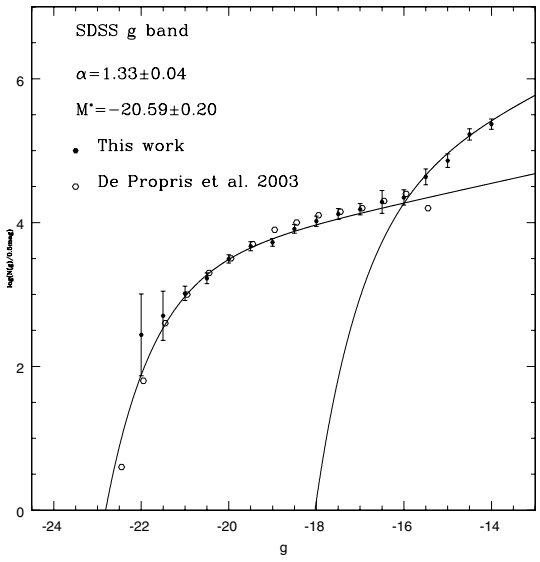

Fig. 14. The Composite LF calculated with the prescription of Colless (1989) with a global background correction and within 1.5 Mpc h^{-1} in the g band (filled points) and the De Propris et al. (2003) Composite LF in the b band derived from the 2df spectroscopic data (empty points).

Goto et al. (2002b) in all the Sloan wavebands. In conclusion, if we exclude the works of Garilli et al. (1999), Paolillo et al. (2001) and Goto et al. (2002b) from our analysis, the range of α is reduced significantly to the values between –1.50 and –1.22. All the values of the slope of our g band composite LF perfectly fit in this range of results.

5.4. Comparison with the field

One of the most important and interesting aspects of the luminosity function is the comparison of the LFs derived in different environments. The SDSS field luminosity function is given by Blanton et al. (2003). In this work the absolute magnitude limit is around $-16+5\log(h)$ in the g and r bands and $-17+5\log(h)$ in the i and z bands. Therefore, the field LF is not studied in the magnitude range of the dwarf galaxies. We compare, then, only the bright end of the cluster luminosity function with the SDSS field LF. The result of the comparison with the field LF of Blanton et al. (2003) is that the field LF is systematically flatter than the cluster LF in any band, while the cluster M^* is brighter than the field M^* of about 0.5 mag. However, there is not an overall agreement in the literature about the values of slope and M^* in the field luminosity function. As Table 3 shows, most of the results reveal a very poor agreement only within 3σ, while several values (see, e.g., the CfA2 LF of Marzke et al. 1994) do not agree at all with the results of the other surveys. For example, if we compare our cluster lf with the 2df field lf, we should conclude, in agreement with De Propris et al. (2002), that the slope of the cluster lf is consistent with the field lf, while the characteristic magnitute is about 0.5 mag brighter than the field M^*. In conclusion, the rather large scatter of the results in the literature does not allow us to a conclusive comparison between the luminosity function of different environments.

Since the magnitude range of our faint end cluster LF is not covered by the SDSS field LF, we have to compare our results with other surveys. Loveday (1997) in the Stromlo-APM survey finds that the number of faint galaxies seen in projection on the sky is much larger than expected for a flat faint-end Schechter function. Moreover, they show that the best fit function for the field luminosity function is a "double

Table 3. Schechter parameters fitted to the Composite LF retrieved from the literature.

Survey		band	$m_{\rm lim}$	M^*	α	ϕ^* ($\times 10^{-2}\,h^3$ Mpc^{-1})	evolution correction	Reference
AUTOFI		b_j	–14	-19.30 ± 0.13	-1.16 ± 0.05	2.45 ± 0.35	no	(1)
Stromlo-APM		b_j	–15	-19.50 ± 0.13	-0.97 ± 0.15	1.40 ± 0.17	no	(2)
SSRS2		$m_{B(0)}$	–14	-19.45 ± 0.08	-1.16 ± 0.07	1.09 ± 0.30	no	(3)
CfA2		m_Z	–16.5	-18.8 ± 0.3	-1.0 ± 0.2	$4. \pm 1$	no	(4)
EPS	all	b_j	–12.4	-19.61 ± 0.06	-1.22 ± 0.06	2.0 ± 0.4	no	(5)
	early type	b_j	–12.4	-19.62 ± 0.09	-0.98 ± 0.09	1.1 ± 0.2	no	
	late type	b_j	–12.4	-19.47 ± 0.10	-1.40 ± 0.09	1.0 ± 0.2	no	
2dF	all	b_j	–13	-19.79 ± 0.04	-1.19 ± 0.01	1.59 ± 0.14	no	(6)
	early type	b_j	–17	-19.58 ± 0.05	-0.54 ± 0.02	0.99 ± 0.05	no	
	late type	b_j	–13	-19.15 ± 0.05	-1.50 ± 0.03	0.24 ± 0.02	no	
2dF		b_j	–16.5	-19.66 ± 0.07	-1.21 ± 0.03	1.61 ± 0.08	yes	(7)
LCRS		r	–17.5	-20.29 ± 0.02	-0.70 ± 0.05	1.9 ± 0.1	no	(8)
CNOC2	early type	$R_{\rm C}$	–17	-20.50 ± 0.12	-0.07 ± 0.14	1.85 ± 0.37	yes	(9)
	late type	$R_{\rm C}$	–16	-20.11 ± 0.18	-1.34 ± 0.12	0.56 ± 0.30	yes	
SDSS		$u^{0.1}$	–15.54	-17.93 ± 0.03	-0.92 ± 0.07	3.05 ± 0.33	yes	(10)
DR1		$g^{0.1}$	–16.10	-19.39 ± 0.02	-0.89 ± 0.03	2.18 ± 0.08	yes	
		$r^{0.1}$	–16.11	-20.44 ± 0.01	-1.05 ± 0.01	1.49 ± 0.04	yes	
		r	–16.11	–20.54	–1.15	1.77	no	
		$i^{0.1}$	–17.07	-20.82 ± 0.02	-1.00 ± 0.02	1.47 ± 0.04	yes	
		$z^{0.1}$	–17.34	-21.18 ± 0.02	-1.08 ± 0.02	1.35 ± 0.04	yes	

References: (1) Loveday et al. (1992); (2) Ellis et al. (1996); (3) Marzke & Da Costa (1997); (4) Marzke et al. (1994); (5) Zucca et al. (1997); (6) Madgwick et al. (2002); (7) Norberg et al. (2002); (8) Lin et al. (1996); (9) Lin et al. (1999); (10) Blanton et al. (2003).

power-law" Schechter function. Lin et al. (1996) finds in the Las Campana Redshift Survey (LCRS) that the Schechter function is a good approximation of the magnitude range $-23 \leq M_r - 5\log(h) \leq -15.5$ for the field LF, but there is a significant excess relative to the Schechter fit at the faint end $M_r \geq -17.5$. Zucca et al. (1997) finds a steepening of the field LF at $M_{\rm b_J} \leq -17.5 + 5\log(h)$ from the ESO Slice Project (ESP) galaxy redshift survey. A Schechter function is an excellent representation of their data points at $M_{\rm b_J} \leq -16 + 5\log(h)$, but at fainter magnitude it lies below all the points down to $M_{\rm b_j} = -12.4 + 5\log(h)$. They find that the best fit to the data is a two-law fit given by a Schechter function plus a power law with slope –1.5. They conclude that the faint end steepening is almost completely due to galaxies with emission lines. In fact, dividing the galaxies in two samples (i.e. galaxies with and without emission lines) they find very significant differences in their luminosity functions. Galaxies with emission lines show a significantly steeper faint end slope and a slightly fainter M^*. However, it is noteworthy that in their results the Schechter function is a inadequate fit especially for the galaxies without emission lines, which show a significant evidence of an upturn in the dwarf region, while the LF of galaxies with emission lines is much more compatible with a steep Schechter function. A similar difference in the best fit parameters of galaxies with and without emission lines has been found also in the LCRS, Lin et al. (1996), although for each subsample their best fit is significantly flatter than the corresponding slope in the EPS survey.

A partially different result comes from the 2dF survey, which shows for the first time significant evidence for the presence of a substantial passive dwarf population. In fact, Madgwick et al. (2002) find that the Schechter function provides an inadequate fit of the LF calculated over the magnitude range $-22 \leq M_{\rm b_J} - 5\log(h) \leq -13$, especially for the most passive and star-forming galaxies. They conclude that a Schechter function is not a good fit to the data over the entire $M_{\rm b_J}$ magnitude range and that this is mostly due to an overabundance of the faint passive star-forming galaxies relative to the bright objects. In fact, their sample of passive galaxies clearly show a very significant increase in the predicted number density of faint galaxies. Moreover, they argue that the small size of the other surveys has meant that only a statistically insignificant number of galaxies have contributed to the faint magnitude range. Hence previous studies could not determine if the features observed at the faint end were real or a consequence of the small volume being sample at these magnitudes.

Our results are more in agreement with the results of the ESP survey of Zucca et al. (1997). As mentioned in Sect. 5.2, the faint end of our clusters should be due to a significant number of very faint late type galaxies in clusters, which should be compatible with the emission line galaxies observed by Zucca et al. (1997). There is also a qualitative good agreement with the results of the 2dF survey of Madgwick et al. (2002), since the late type galaxies in their sample seem to have a steeper LF than the early type galaxies, even if they conclude that the incompatibility of a Schechter function with the global field LF

should be due to the passive galaxies. However, it is important to stress that we can compare only qualitatively our cluster LF with the field LF retrieved from the literature since we are using different wavebands and we are covering different magnitude range. Therefore, a quantitative comparison between the different environments requires absolutely the measure of the field luminosity function in the Sloan waveband and in the faint magnitude region.

6. Conclusion

The main conclusions of our analysis are as follows:

- we determine the composite LF of galaxies in clusters from the SDSS data. The LF clearly shows a bimodal behavior with an upturn and a evident steepening in the faint magnitude range in any SDSS band. The LF is well fitted by the sum of two Schechter functions. The results are confirmed by different methods of background subtraction. The observed upturn of the faint galaxies has a location ranging from $-16+5\log(h)$ in the g band to $-18.5+5\log(h)$ in the z band.
- The bright end LF shows the classical slope of –1.25 in each photometric band, while M^* is brighter in the red bands than in the blue bands. The distribution of the Schechter parameters obtained fitting only the bright end of the individual cluster LF is close to a Gaussian around the corresponding value of the composite bright-end LF. We check the dependence of the Schecter parameters of the composite LF on the clustercentric distance calculating the LF within different cluster apertures. We do not find any significant variation of the results with different apertures. Therefore, we conclude that the bright-end of the galaxy clusters is universal in different cluster environments, both in different systems and in different locations within the same cluster.
- The faint end LF is much steeper than the bright end LF with slope $-2.5 \leq \alpha \leq -1.6$. We apply different tests to check whether the observed faint end in the single clusters is due to the presence of background large scale structures or a second cluster on the line of sight. To check the first possibility we measure the individual cluster LF with a color cut method to identify the cluster members. We obtain the same slope observed with the statistical background subtraction. Moreover, we observe that the faint population is dominated by galaxies with colors compatible with late type galaxies at the cluster redshift. We then conclude that the observed steepening of the cluster LF is due to the presence of a real population of faint cluster galaxies.
- We defined the Dwarf to Giant galaxy Ratio DGR as the ratio between the number of galaxies in the magnitude range $-18 \leq M \leq -16.5$ and the number of galaxies brighter than –20 mag. In each waveband the DGR seems to slightly increase from the center 0.3 Mpc h^{-1} to 1.0 Mpc h^{-1}. The distribution of DGR of the single clusters has a peak around the value predicted by the composite bright-end and and a large spread at larger values. We check the relation between the DGR and the cluster richness and between the DGR and M^* through the Spearman rank coefficient and we do not find any correlation between the parameters. However DGR(z) clearly anti-correlates with both the X-ray and the optical cluster luminosities. The anti-correlation between cluster DGRs and cluster luminosities is most likely due to the choice of a fixed metric aperture for all the clusters. Therefore, because of this effect, the different cluster physical sizes must be taken into account before any conclusion about the universality of the shape of the cluster faint end LF is reached.

We compare the above results with the field LF calculated in the Sloan Digital Sky Survey and in other surveys. The magnitude range covered by the SDSS field LF allows us to compare only the bright end of the cluster luminosity function with the field LF. Unfortunately there is no good agreement between the results retrieved in the literature. Therefore we cannot perform a conclusive comparison between the LF of the different environments. Moreover, several surveys find evidence for the presence of an upturn at the faint end of the field luminosity function in agreement with our results for the cluster LF. In particular Zucca et al. (1997) find in the ESP field LF evidence for the presence of a late type galaxy population dominating the faint end of the field luminosity function. However, it is important to stress that this is only a qualitative comparison and does not allow us to draw any conclusion about the nature of the faint population in clusters and in the field. We can only conclude that the faint end of the cluster LF is systematically steeper than the field LF, although the field LF seems to show some evidence of an excess of galaxies in the faint magnitude range relative to a Schechter function.

Hierarchical clustering theories of galaxy formation generally predict a steep mass function of galactic halos (Kauffmann et al. 1993; Cole et al. 1994). This is in conflict with the flat galaxy LF measured in the field and in diffuse local groups, but not with the steep LF measured in many clusters. However in the hierarchical universe, clusters form relatively recently from the accretion of smaller systems. The dynamical processes that operate in clusters are destructive. Ram pressure stripping (e.g. Moore & Bauer 1999) and gravitational tides/galaxy harassment (e.g. Moore et al. 1996, 1998) will tend to fade galaxies by removing gas or stripping stars. These processes are most effective for less massive, less bound systems. Hence, we might expect to see a flattening of the faint end slope in clusters compared to the field, rather than the observed steepening.

Understanding the nature of the observed faint galaxy population requires a more detailed study of the galaxy population in the clusters through the analysis of the morphological type, the colors and the study of the relation between the fraction of dwarf galaxies and the cluster parameters such as the cluster mass, velocity dispersion or the X-ray luminosity. Moreover, the origin of this faint population can be understood only if a conclusive comparison between cluster and field is possible. At the moment, as we discussed above, the SDSS field LF based on the Sloan spectroscopic galaxy sample does not allow to an exhaustive comparison and analysis of the different environments.

It is clear from our results and from the existing work in the literature that the composite bright end of the cluster LF can

give useful information on the global cluster properties (such as the total optical luminosity, which is dominated by the very bright cluster galaxies), but it does not provide useful information on the cluster galaxy population as a whole. Equally it is clear that a Schechter function is a good fit of the cluster LF only in a very restricted magnitude range (the bright end). The photometric data available now should make it possible to consider non-parametric comparisons between the individual and the composite cluster LFs using the full range of the available data. Our results on the dwarf galaxy fraction are a first step in this direction, but it should be possible to devise a test that does not require a split in bright and faint galaxies but considers the cluster galaxy population as a whole.

Acknowledgements. We would like to thank the referee, S. Lumsden, for the useful comments which significantly improved the paper.
Funding for the creation and distribution of the SDSS Archive has been provided by the Alfred P. Sloan Foundation, the Participating Institutions, the National Aeronautics and Space Administration, the National Science Foundation, the U.S. Department of Energy, the Japanese Monbukagakusho, and the Max Planck Society. The SDSS Web site is `http://www.sdss.org/`. The SDSS is managed by the Astrophysical Research Consortium (ARC) for the Participating Institutions. The Participating Institutions are The University of Chicago, Fermilab, the Institute for Advanced Study, the Japan Participation Group, The Johns Hopkins University, Los Alamos National Laboratory, the Max-Planck-Institute for Astronomy (MPIA), the Max-Planck-Institute for Astrophysics (MPA), New Mexico State University, University of Pittsburgh, Princeton University, the United States Naval Observatory, and the University of Washington.

References

Abazajian, K., Adelman, J., Agueros, M., et al. 2003, AJ, 126, 2081 (Data Release One)
Adami, C., Ulmer, M. P., Durret, F., et al. 2000, A&A, 353, 930
Beijersbergen, M., Hoekstra, H., & Van Dokkum, P. G. 2002, MNRAS, 329, 385
Bernstein, G. M., Nichol, R. C., Tyson, J. A., et al. 1995, AJ, 110, 1507
Blanton, M. R., Dalcanton, J., Eisenstein, D., et al. 2001, AJ, 121, 2358
Blanton, M. R., Hogg, D. W., Bahcall, N. A., et al. 2003, ApJ, 592, 819
Böhringer, H., Voges, W., Huchra, J. P., et al. 2000, ApJS, 129, 435
Böhringer, H., Schuecker, P., Guzzo, L., et al. 2001, A&A, 369, 826
Böhringer, H., Collins, C. A., Guzzo, L., et al. 2002, ApJ, 566, 93
Boyce, P. J., Phillips, S., Bryn Jones, J., et al. 2001, MNRAS, 328, 277
Cole, S., Aragon-Salamanca, A., Frenk, C. S., et al. 1994, MNRAS, 271, 781
Colless, M. 1989, MNRAS, 237, 799
Cortese, L. 2003, A&A, 410, L25
Cross, N. J. G., Driver, S. P., Liske, J., et al. 2004, MNRAS, 349, 576
De Grandi, S., Böhringer, H., & Guzzo, L. 1999, ApJ, 514, 148
De Propris, R., Colless, M., Driver, S. P., et al. 2003, MNRAS, 342, 725
Dressler, A. 1978, ApJ, 223, 765
Driver, S. P., Phillips, S., Davies, J. I., et al. 1994, MNRAS, 268, 393
Ellis, R. S., Colless, M., Broadhurst, T., et al. 1996, MNRAS, 280, 235
Fukugita, M., Shimasaku, K., & Ichikawa, T. 1995, PASJ, 107, 945
Fukugita, M., Ichikawa, T., & Gunn, J. E. 1996, AJ, 111, 1748
Garilli, B., Maccagni, D., Stefano, A., et al. 2001, A&A, 342, 408
Goto, T., Sekiguchi, M., Nichol, R. C., et al. 2002a, AJ, 123, 1807
Goto, T., Okamura, S., McKay, T. A., et al. 2002b, PASP, 54, 515
Gunn, J. E., Carr, M. A., Rockosi, C. M., et al. 1998, AJ, 116, 3040 (SDSS Camera)
Hogg, D.W., Finkbeiner, D. P., Schlegel, D. J., & Gunn, J. E. 2001, AJ, 122, 2129
Horner, D. 2001, Ph.D. Thesis, University of Maryland
Kauffmann, G., White, S. D. M., & Guideroni, B. 1993, MNRAS, 264, 201
Kochanek, C. S., Pahre, M. A., Falco, E. E., et al. 2001, ApJ, 560, 566
Lin, H., Kirshner, R. P., Shectman, S. A., et al. 1996, ApJ, 464, 60
Lin, H., Yee, H. K. C., Carlberg, R. G., et al. 1999, ApJ, 518, 533
Loveday, J., Peterson, B. A., Efstathiou, G., et al. 1992, ApJ, 390,338
Loveday, J. 1997, ApJ, 489, 29
Lugger, P. M. 1986, ApJ, 303, 535
Lugger, P. M. 1989, ApJ, 343, 572
Lumsden, S. L., Collins, C. A., Nichol, R. C., et al. 1997, MNRAS, 290, 119
Lupton, R. H., Gunn, J. E., & Szalay, A. S. 1999, AJ, 118, 1406
Lupton, R., Gunn, J. E., Ivezić, Z., et al. 2001, in Astronomical Data Analysis Software and Systems X, ed. F. R. Harnden, Jr., F. A. Primini, & H. E. Payne (San Francisco: ASP), ASP Conf. Ser., 238, 269 [`arXiv:astro-ph/0101420`]
Madgwick, D. S., Lahav, O., Baldry, I. K., et al. 2002, MNRAS, 333, 133
Marzke, R. O., Huchra, J. P., & Geller, M. J. 1994, ApJ, 428,43
Marzke, R. O., & Da Costa, L. N. 1997, AJ, 113, 185
Moore, B., Katz, N., Lake, G., et al. 1996, Nature, 379, 613
Moore, B., lake, G., & Katz, N. 1998, ApJ, 495, 139
Mulchaey, J. S., Davis, D. S., Mushotzky, R. F., & Burstein, D. 2003, ApJS, 145, 39
Norberg, P., Cole, S., Baugh, C. M., et al. 2002, MNRAS, 336, 907
Paolillo, M., Andreon, S., Longo, G., et al. 2001, A&A, 367, 59
Phillips, S., Driver, S. P., Couch, W. J., et al. 1998, ApJ, 498, L119
Popesso, P., Böhringer, H., Brinkmann, J., et al. 2004, A&A, 423, 449
Reiprich, T., & Böhringer, H. 2002, ApJ, 567, 740 (R02)
Retzlaff, J. 2001, XXIst Moriond Astrophysics Meeting, March 10–17, 2001 Savoie, France, ed. D. M. Neumann, & J. T. T. Van
Rauzy, S., Adami, C., Mazure, A., et al. 1998, A&A, 337, 31
Sabatini, S., Davies, J., Scaramella, R., et al. 2003, MNRAS, 341, 981
Schechter, P. 1976, ApJ, 203, 297
Schlegel, D., Finkbeiner, D. P., & Davis, M. 1998, ApJ, 500, 525
Shimasaku, K., Fukugita, M., Doi, M., et al. 2001, AJ, 122, 1238
Smith, R. M., Driver, S. P., Phillips, S., et al. 1997, MNRAS, 287, 415
Smith, J. A., Tucker, D. L., Kent, S. M., et al. 2002, AJ, 123, 2121
Stoughton, C., Lupton, R. H., Bernardi, M., et al. 2002, AJ, 123, 485
Strauss, M. A., Weinberg, D. H., Lupton, R. H., et al. 2002, AJ, 124, 1810
Trentham, N. 1998, MNRAS, 295,360
Ulmer, M. P., Bernstein, G. M., Martin, D. R., et al. 1996, AJ, 112, 2517
Valotto, C., Nicotra, M. A., Muriel, H., et al. 1997, ApJ, 479, 90
Valotto, C., Moore, B., & Lambas, D. 2001, ApJ, 479, 90
Valotto, C., Muriel, H., Moore, B., et al. 2004, ApJ, 479, 90
Yagi, M., Kashikawa, N., Sekiguchi, M., et al. 2002, AJ, 123, 87
Yasuda, N., Fukugita, M. Narayanan, V. K., et al. 2001, AJ, 122, 1104
York, D. G., Adelman, J., Anderson, J. E., et al. 2000, AJ, 120, 1579
Zucca, E., Zamorani, G., Vettolani, G., et al. 1997, A&A, 326, 477